Published in final edited form as:
Chemistry. 2010 September 3; 16(33): 10234–10239. doi:10.1002/chem.201000341.

Facile Synthesis of Ag Nanocubes of 30 to 70 nm in Edge Length with CF_3COOAg as a Precursor

Qiang Zhang[†,‡], **Weiyang Li**[†], **Long-Ping Wen**[‡], **Jingyi Chen**[†], and **Younan Xia**[†,*]

[†]Department of Biomedical Engineering, Washington University, St. Louis, Missouri 63130, USA

[‡]Hefei National Laboratory for Physical Sciences at the Microscale, University of Science and Technology of China, Hefei, Anhui 230027, P. R. China

Abstract

This paper describes a new protocol for producing Ag nanocubes of 30 to 70 nm in edge length with the use of CF_3COOAg as a precursor to elemental silver. By adding a trace amount of sodium hydrosulfide (NaHS) and hydrochloric acid (HCl) into the polyol synthesis, Ag nanocubes were obtained with good quality, high reproducibility, and on a scale up to 0.19 g per batch for the 70-nm Ag nanocubes. The Ag nanocubes were found to grow in size at a controllable pace over the course of synthesis. The linear relationship between the edge length of the Ag nanocubes and the position of localized surface plasmon resonance (LSPR) peak provides a simple method for finely tuning and controlling the size of the Ag nanocubes by monitoring the UV-vis spectra of the reaction at different times.

Keywords

CF_3COOAg; Ag nanocube; size control

Introduction

In recent years, there has been a continuous, strong effort in shape-controlled synthesis of silver nanostructures because of their remarkable properties and exciting applications in areas such as photonics, electronics, catalysis, sensing, and biomedicine.[1–8] Silver nanocubes stand out from various types of Ag nanostructures[9] (e.g., spheres, rods, bars, belts and wires) due to their sharp corners/edges, uniform size, and superior performance in a range of applications involving localized surface plasmon resonance (LSPR),[10–12] surface-enhanced Raman scattering (SERS),[13–17] biosensing.[18,19] Silver nanocubes have also been used as a sacrificial template to generate gold, palladium, and platinum nanoboxes or nanocages,[20] which have started to show great potential in catalysis,[21] contrast enhancement in biomedical imaging,[22,23] photothermal therapy[24] and drug delivery.[25] All of these applications require us to produce Ag nanocubes in high quality and relatively large quantity. In order to meet this challenge, we and other groups have developed a number of methods to produce Ag nanocubes, with notable examples including polyol reduction,[26–28] hydrothermal process,[29,30] epitaxial growth on Au octahedronal seeds,[31] and ATP-mediated reduction in a polymer matrix.[32] However, most of these protocols have shortcomings in terms of reaction time, size control, yield, quantity, as well as reproducibility.

*Corresponding author: xia@biomed.wustl.edu.

In the pursuit of a superior method, we recently started to switch to a new silver precursor, CF_3COOAg, instead of the $AgNO_3$ widely used in previous work. Our argument was that the nitrate group may decompose at an elevated temperature typical of a polyol synthesis to generate ionic and/or gaseous species, making the synthesis more difficult to understand and control. In comparison, the trifluoroacetate group is more stable. With this new precursor, we found that the presence of trace amounts of NaHS and HCl were necessary for the production of high-quality Ag nanocubes with sizes ranging from 30 to 70 nm. Compared with the previously reported methods for the preparation of Ag nanocubes,[26–32] this new protocol offers at least three significant advantages: *i*) the reaction rate is in an appropriate range, allowing us to control and fine-tune the size of Ag nanocubes by following the synthesis with UV-vis spectroscopy; *ii*) the synthesis becomes essentially not sensitive to the manufacturing source of ethylene glycol (EG), improving both the robustness and reproducibility of the polyol synthesis; and *iii*) it is relatively simple and straightforward to scale up the synthesis to produce Ag nanocubes in relatively large quantities and with high quality.

Results and discussion

Figure 1 shows transmission electron microscopy (TEM) images of the Ag nanocubes obtained at different stages of a typical synthesis: 15, 30, 60, and 90 min, respectively, after the addition of CF_3COOAg. During this period of time, the edge length of the nanocubes was increased from 30 to 42, 50, and 70 nm. The relatively slow growth rate allowed us to conveniently control and thus routinely tune the size of the Ag nanocubes by quickly taking UV-vis spectra from small aliquots sampled from the reaction solution. This new capability is a significant advantage over previously reported methods. For example, with respect to the NaHS-mediated polyol synthesis, the reaction was typically completed in 8–10 min and it only took about 2 min for the Ag nanocubes to grow from 25 to 45 nm.[26,33] This short period of time makes it very difficult to follow the increase of size using a UV-vis spectroscopic method. As a result, we could only obtain Ag nanocubes of different sizes by monitoring the color changes associated with the nanocubes as they were growing,[26,33] which was too vague to obtain Ag nanocubes having specific sizes. On the other extreme, the HCl-mediated polyol synthesis usually took 16 to 25 h to complete,[27] making it less practical to control the size of the Ag nanocubes by constantly monitoring the changes to UV-vis spectra.

In the present synthesis, the Ag nanocubes grew from 30 to 70 nm when the reaction time increased from 15 min to 90 min. As a result, we could easily take a small amount (several drops) of the reaction solution with a glass pipette, diluted with DI water in a cuvette, followed by recording of its UV-vis extinction spectrum. All of these could be completed in 1–2 min, during which the Ag nanocubes grew very little in size. Significantly, we also found that the synthesis was sufficiently robust so that frequent removal of the stopper from the flask had a minor impact on the path and yield of the reaction. Taken together, we could finely control the sizes of resultant Ag nanocubes according to their LSPR peak positions. To better understand the relationship between the sizes and the LSPR peak positions of Ag nanocubes, we analyzed the UV-vis spectra of Ag nanocubes with different edge lengths that were obtained from the syntheses described in Figure 1. As shown in Figure 2A, the major LSPR peaks of the Ag nanocubes displayed a continuous red-shift along with the size increase. When the edge length of the Ag nanocubes was increased from 30 to 42, 50, and 70 nm, the positions of the major LSPR peaks were located at 420, 436, 449, and 474 nm, respectively. The plot in Figure 2B suggests that there was a more or less linear relationship between the LSPR peak position and the edge length of the Ag nanocubes. The equation for describing the calibration curve was $\lambda_{max} = 1.3927\ \ell + 378.25$ ($R^2 = 0.99$), where λ_{max} and ℓ are the peak position and edge length, respectively. In practice, this calibration curve should

allow one to obtain Ag nanocubes of a specific edge length by monitoring the UV-vis spectra of the reaction solution.

To achieve a better understanding of the growth mechanism, aliquots were also taken from the early stages (<15 min) of a standard synthesis and then analyzed by TEM and high-resolution TEM. Immediately after the addition of CF_3COOAg, the solution went into a whitish color, followed by the appearance of a slight yellow color in 1 min. As shown by the TEM image in Figure 3A, there were two sizes of nanoparticles co-existing in the product sampled at t = 1 min; the big nanoparticles had an average size of 57 nm while the small ones were around 13 nm in diameter. The high-resolution TEM image taken from a small particle gave a lattice fringe spacing of 2.0 Å (inset of Fig. 3A), which is consistent with the {200} lattice spacing of face-centered cubic (*fcc*) Ag.[33] This information suggests that some of the small particles were single crystalline and made of Ag, which could serve as seeds and eventually grow into nanocubes under the influence of poly(vinyl pyrrolidone) (PVP). As a capping agent, PVP is able to selectively bind to the {100} facets of Ag nanocrystals, favoring the formation of nanocubes when the seeds are single crystalline.[9] In the present case, the molar ratio of PVP to CF_3COOAg had to be higher than 2:1 in order to obtain Ag nanocubes in high yields. Energy-dispersive X-ray spectroscopy (EDX) analysis of the big nanoparticles gave an Ag-to-Cl atomic ratio of 50:45, indicating that these particles were made of AgCl. These results suggest that the formation of AgCl nanoparticles and the birth of Ag nanocrystal seeds both occurred at t < 1 min. After this point, the color of the reaction solution started darkening from slight yellow to deep orange. As shown in Figure 3, B–F, the number and size of AgCl nanoparticles decreased with the reaction time, accompanied by an increase for Ag nanocrystals in terms of both density and size. Eventually, Ag nanocubes started to appear in the solution around t = 11 min (Figure 3E).

In order to obtain Ag nanocubes in high yields and with good quality, we optimized the synthesis by adjusting the concentrations of both NaHS and HCl. As shown in Figure 4, each column showed the reactions performed under the same concentration of NaHS; from left to right, the concentration of NaHS was doubled from 0.125 to 0.25 and 0.50 μM. Each row showed the reactions performed under the same concentration of HCl; from top to bottom, the concentration of HCl was doubled from 0.105 to 0.21 and 0.42 mM. All the reactions were stopped at t = 30 min after the introduction of CF_3COOAg. It is clear that the concentration of NaHS was a less important factor relative to the concentration of HCl as Ag nanocubes of good quality could be obtained in a range of NaHS concentrations (Fig. 4, A–C). From top to bottom, the size of Ag nanocubes became larger along with the increase of HCl concentration. For both concentrations of 0.105 and 0.21 mM, we could obtain Ag nanocubes of good quality (Fig. 4, A and D). When the concentration of HCl was increased to 0.42 mM, there were also some other types of particles in the products, including bipyramids, multiply twinned nanorods, irregular particles, in addition to the Ag nanocubes. Taken together, we found that the best result was obtained when the concentrations of NaHS and HCl were 0.25 μM and 0.21 mM, which represents the standard procedure used in this paper.

As shown in Figure 4, both NaHS and HCl had to be introduced into the synthesis when CF_3COOAg was employed as a precursor to Ag nanocubes. In order to investigate the roles that NaHS or HCl played in this new protocol, we performed the synthesis with different combinations of reagents. The samples were collected at t = 1 and 30 min after the introduction of CF_3COOAg, and then analyzed by TEM. As shown in Figure 5A, multiply twinned nanoparticles were obtained in the sample taken at t = 1 min of the synthesis when both NaHS and HCl were absent, and these particles then agglomerated into larger particles with irregular shapes at t = 30 min (Fig. 5B). Upon the addition of NaHS (Fig. 5C), there

were 28% single-crystal nanoparticles with an average size of 14 nm co-existing with multiply twinned nanoparticles in the sample taken at t = 1 min. In this case, Ag_2S clusters formed in the reaction solution could serve as primary nucleation sites to catalyze the reduction of CF_3COOAg and thus formation of single-crystal Ag seeds.[26] The observation of single-crystal Ag seeds suggested that NaHS played the same role as in the previous work. After 30 min into the reaction (Fig. 5D), the small nanoparticles evolved into a mixture of agglomerated nanoparticles, nanorods, and a few single-crystal nanospheres and bipyramids. If HCl instead of NaHS was present (Fig. 5E), there were some cubic nanostructures with an average size of 57 nm observed in the sample. Our EDX analysis suggested that the chemical composition of these nanocubes was AgCl, which was consistent with the result reported in the HCl-mediated synthesis of Ag nanocubes.[27] The product sampled at t = 30 min consisted of irregular nanoparticles, nanorods, and a few nanocubes (Fig. 5F). However, if CF_3COOAg solution was titrated into the reaction solution at a rate of 0.07 mL per min by using syringe pump, the product mainly consisted of Ag nanocubes, together with few nanorods and other irregular nanoparticles (Fig. S1). These results suggest that both NaHS and HCl are critical to the successful synthesis of Ag nanocubes.

Our previous studies suggested that a combination of an oxidatant and a ligand could result in a powerful oxidative etchant to selectively remove multiply twinned Ag seeds from a polyol synthesis.[34] The O_2 from air and Cl^- ions (from NaCl or HCl) has been validated as a typical example for generating single-crystal seeds and thus Ag nanocubes.[35] In order to verify this mechanism, we performed the synthesis under argon, with other conditions being the same as the standard procedure. As shown in Figure 5G, the product sampled at t = 1 min was similar to the sample taken from the standard synthesis (Fig. 3A). However, after 30 min into the reaction under argon, the majority of the product was Ag nanocubes, together with a small amount of nanorods and irregular nanoparticles (Fig. 5H). This observation suggests that oxidative etching only played a minor role in the formation of single-crystal seeds and Ag nanocubes in the presence of NaHS. In this case, the control over product morphology was mainly provided by Ag_2S seeds formed at the very beginning of a synthesis. Of course, the presence of Cl^- and O_2 could help to remove the small number of twinned seeds that might also form parallel to the Ag_2S-mediated nucleation process. As shown in Figure 3C, there were also some twinned seeds co-existing with single-crystal ones, but the final product only consisted of single-crystal nanocubes, indicating that the oxidative etching by O_2/Cl^- was also involved in the synthesis conducted in air.

The synthesis was further optimized by adjusting the reaction temperature. As shown in Figure 6 A and B, the synthesis was also performed at both 130 and 170 °C with other parameters being the same as the standard procedure. At these two temperatures, we obtained a mixture of Ag nanocubes and other types of nanoparticles, suggesting that the temperature of 150 °C used for the standard procedure seemed to be the optimal condition. To distinguish the roles of proton and chloride ions, HCl was replaced by NaCl for the standard synthesis. As shown in Figure 6C, there was no significant difference between the products obtained with either HCl (standard procedure) or NaCl. This observation indicates that protons were not a necessarily critical component in this synthesis. This is not surprising because protons are supposed to be generated during polyol reduction. To evaluate the capability of this new protocol for potential high-volume production of Ag nanocubes, we performed a scalp-up synthesis which used CF_3COOAg at an amount of 20 times of the standard procedure, and we could still obtain Ag nanocubes of good quality in high yield (Fig. 6D).

For most applications, it is also important to find a simple and reliable way to store Ag nanocubes with good preservation of morphology for a relatively long period of time. As

shown in Figure S2, freshly prepared Ag nanocubes could be stored on a solid support (in a dry state) for three months without losing their sharp corners and edges. In comparison, the Ag nanocubes became rounded at corners and edges when they were stored in de-ionized (DI) water for three months. We also found that the Ag nanocubes stored in the dry state could be easily re-dispersed in DI water via brief sonication.

Conclusion

In summary, Ag nanocubes with edge length from 30 to 70 nm were synthesized in large quantities by introducing CF_3COOAg as a new silver precursor into the polyol synthesis. It was found that both NaHS and HCl were necessary to the production of Ag nanocubes with uniform shape, narrow size distribution, and high reproducibility. The results indicated that NaHS played an important role in the formation of single-crystal seeds, and Cl^- ions acted as a ligand for oxidative etching to eliminate twinned particles. The relatively growth pace of Ag nanocubes over the course of synthesis and the linear relationship between the position of the LSPR peak and the edge length of the cubes make it easy to control and finely tune the size of every batch of Ag nanocubes by monitoring the UV-vis spectra. Another advantage of this method is that the reproducibility of the reaction and the quality of Ag nanocubes were not sensitive to the manufacturing source of EG, which was usually a major problem for the polyol synthesis of Ag nanocubes.

Experimental Section

Sythesis of Ag nanocubes

In a standard synthesis, 5 mL ethylene glycol (EG, J. T. Baker, lot no. G32B27) was added into a 100-mL round bottom flask (ACE Glass) and heated under magnetic stirring in an oil bath pre-set to 150 °C. 0.06 mL NaHS (3 mM in EG, Aldrich, 02326AH) was quickly injected into the heated solution after its temperature had reached 150 °C. Two minutes later, 0.5 mL of a 3 mM HCl solution was injected into the heated reaction solution, followed by the addition of 1.25 mL of poly(vinyl pyrrolidone) (PVP, 20 mg/mL in EG, MW≈55,000, Aldrich). The HCl solution was prepared by adding 2.5 μL HCl (38% by weight) into 10.30 mL EG. After another 2 min, 0.4 mL silver trifluoroacetate (CF_3COOAg, 282 mM in EG, Aldrich, 04514TH) was added into the mixture. During the entire process, the flask was capped with a glass stopper except during the addition of reagents. After the addition of CF_3COOAg, the transparent reaction solution took a whitish color and quickly became slightly yellow in 1 min, indicating the formation of the Ag seeds. The reaction was allowed to proceed for different periods of time and its color went through three stages of dark red, reddish grey, and brown as the edge length of the Ag nanocubes increased. The reaction solution was quenched by placing the reaction flask in an ice-water bath. All the samples were collected by centrifugation and then washed with acetone once to remove the remaining precursor and EG, and then DI water four times to remove excess PVP. We controlled the sizes of the Ag nanocubes monitoring their main LSPR peak positions using a UV-vis spectrometer from 15 to 90 min with an interval of 15 min. Briefly, a small amount (a few drops) of the reaction solution was taken out from the flask using a glass pipette and diluted with 1 mL DI water in a cuvette, followed by recording its extinction spectrum and compared with the calibration curve for wavelength versus edge length.

Scale-up synthesis of Ag nanocubes

The scale-up synthesis of Ag nanocubes was carried out by following the procedure for the standard synthesis, except that the amounts of all reagents were increased by 20 times (or other different times). For example, 100 mL EG was added into a 250-mL round bottom flask (ACE Glass) and heated under magnetic stirring in an oil bath pre-set to 150 °C. After

the temperature of the oil bath had reached 150 °C, 1.2 mL of the 3 mM NaHS solution and 2 min later, 10 mL of the 3 mM HCl was injected, followed by the addition of 25 mL of the PVP solution. After another 2 min, 8 mL of the CF_3COOAg solution was introduced. The flask was capped with a glass stopper except during the addition of reagents. The procedures for size control and sample collection were the same as the standard synthesis.

Instrumentation

The samples for transmission electron microscopy (TEM) were prepared by dropping 1.5 μL of the aqueous suspension onto a carbon-coated copper grid. The TEM images were captured using a microscope (FEI G2 Spirit Twin) operated at 120 kV. High-resolution TEM images were obtained using a JEOL 2100F operated at 200 kV. The energy-dispersive X-ray (EDX) spectra were captured using a field emission microscope (FEI, Nova NanoSEM 230) operated at accelerating voltages of 10–20 kV. The UV-vis spectra were taken using a Cary 50 spectrophotometer (Palo Alto, CA).

Supplementary Material

Refer to Web version on PubMed Central for supplementary material.

Acknowledgments

This work was supported in part by a 2006 Director's Pioneer Award from the NIH (DP1 OD000798) and startup funds from Washington University in St. Louis. As a visiting student from the University of Science and Technology of China, Q.Z. was also partially supported by the China Scholarship Council. Part of the work was performed at the Nano Research Facility (NRF), a member of the National Nanotechnology Infrastructure Network (NNIN) supported by the NSF under award no. ECS-0335765.

References

[1]. Jin R, Cao Y, Mirkin CA, Kelly KL, Schatz GC, Zheng JG. Science. 2001; 294:1901. [PubMed: 11729310]

[2]. Braun E, Eichen Y, Sivan U, Ben-Yoseph G. Nature. 1998; 391:775. [PubMed: 9486645]

[3]. Wiley BJ, Im SH, Li Z-Y, McLellan J, Siekkinen A, Xia Y. J. Phys. Chem. B. 2006; 110:15666. [PubMed: 16898709]

[4]. Sun J, Ma D, Zhang H, Liu X, Han X, Bao X, Weinberg G, Pfänder N, Su D. J. Am. Chem. Soc. 2006; 128:15756. [PubMed: 17147385]

[5]. Tao A, Kim F, Hess C, Goldberger J, He R, Sun Y, Xia Y, Yang P. Nano Lett. 2003; 3:1229.

[6]. Gunawan C, Teoh WY, Marquis CP, Lifia J, Amal R. Small. 2003; 5:341. [PubMed: 19152359]

[7]. Fang H, Wu Y, Zhao J, Zhu J. Nanotechnology. 2006; 17:3768.

[8]. McFarland AD, Duyne RPV. Nano Lett. 2003; 3:1057.

[9]. Wiley B, Sun Y, Mayers B, Xia Y. Chem.- A European J. 2004; 11:454.

[10]. Mock JJ, Smith DR, Schultz S. Nano Lett. 2003; 3:485.

[11]. Sherry LJ, Chang S, Schatz GC, Duyne PV. Nano Lett. 2005; 5:2034. [PubMed: 16218733]

[12]. Krenn JR. Nat. Mater. 2003; 2:210. [PubMed: 12690387]

[13]. Li W, Camargo PHC, Lu X, Xia Y. Nano Lett. 2009; 9:485. [PubMed: 19143509]

[14]. Yang Y, Matsubara S, Xiong L, Hayakawa T, Nogami M. J. Phys. Chem. C. 2007; 111:9095.

[15]. Tran ML, Centeno SP, Hutchison JA, Engelkamp H, Liang D, Tendeloo GV, Sels BF, Hofkens J, Uji-I H. J. Am. Chem. Soc. 2008; 130:17240. [PubMed: 19049275]

[16]. Lu Y, Liu GL, Lee LP. Nano Lett. 2005; 5:5. [PubMed: 15792403]

[17]. Mahmoud MA, Tabor CE, El-Sayed MA. J. Phys. Chem. C. 2009; 113:5493.

[18]. Anker JN, Hall WP, Lyandres O, Shah NC, Zhao J, Duyne RPV. Nat. Mater. 2008; 7:442. [PubMed: 18497851]

[19]. Galush WJ, Shelby SA, Mulvihill MJ, Tao A, Yang P, Groves JT. Nano Lett. 2009; 5:2077. [PubMed: 19385625]

[20]. Skrabalak SE, Chen J, Sun Y, Lu X, Au L, Cobley CM, Xia Y. Acc. Chem. Res. 2008; 41:1587. [PubMed: 18570442]

[21]. Zeng J, Zhang Q, Chen J, Xia Y. Nano Lett. 2010; 10:30. [PubMed: 19928909]

[22]. Yang X, Skrabalak SE, Li Z-Y, Xia Y, Wang LV. Nano Lett. 2007; 7:3798. [PubMed: 18020475]

[23]. Tong L, Cobley CM, Chen J, Xia Y, Cheng J-X. Angew Chem. Int. Ed. 2010 in press.

[24]. Chen J, Glaus C, Laforest R, Zhang Q, Yang M, Gidding M, Welch MJ, Xia Y. Small. 2010 in press.

[25]. Yavuz M, Cheng Y, Chen J, Cobley CM, Zhang Q, Rycenga M, Xie J, Kim C, Song KH, Schwartz AG, Wang LV, Xia Y. Nat. Mater. 2009; 8:935. [PubMed: 19881498]

[26]. Siekkinen AR, McLellan JM, Chen J, Xia Y. Chem. Phys. Lett. 2006; 432:491. [PubMed: 18496589]

[27]. Im SH, Lee YT, Wiley B, Xia Y. Angew. Chem. Int. Ed. 2005; 44:2154.

[28]. Tao A, Sinsermsuksakul P, Yang P. Angew. Chem. Int. Ed. 2006; 45:4597.

[29]. Yu D, Yam VW. J. Am. Chem. Soc. 2004; 126:13200. [PubMed: 15479055]

[30]. Chen H, Wang Y, Dong S. Inorg. Chem. 2007; 46:10587. [PubMed: 17999489]

[31]. Fan F, Liu D, Wu Y, Duan S, Xie Z, Jiang Z, Tian Z. J. Am. Chem. Soc. 2008; 130:6949. [PubMed: 18465860]

[32]. Zhang Q, Huang CZ, Ling J, Li YF. J. Phys. Chem. B. 2008; 112:16990. [PubMed: 19367987]

[33]. Zhang Q, Cobley CM, Au L, Mckiernan M, Schwartz A, Wen LP, Chen J, Xia Y. Appl. Mater. Interfaces. 2009; 1:2044.

[34]. Xia Y, Xiong Y, Lim B, Skrabalak SE. Angew. Chem. Int. Ed. 2009; 48:60.

[35]. Wiley B, Herricks T, Sun Y, Xia Y. Nano Lett. 2004; 4:1733.

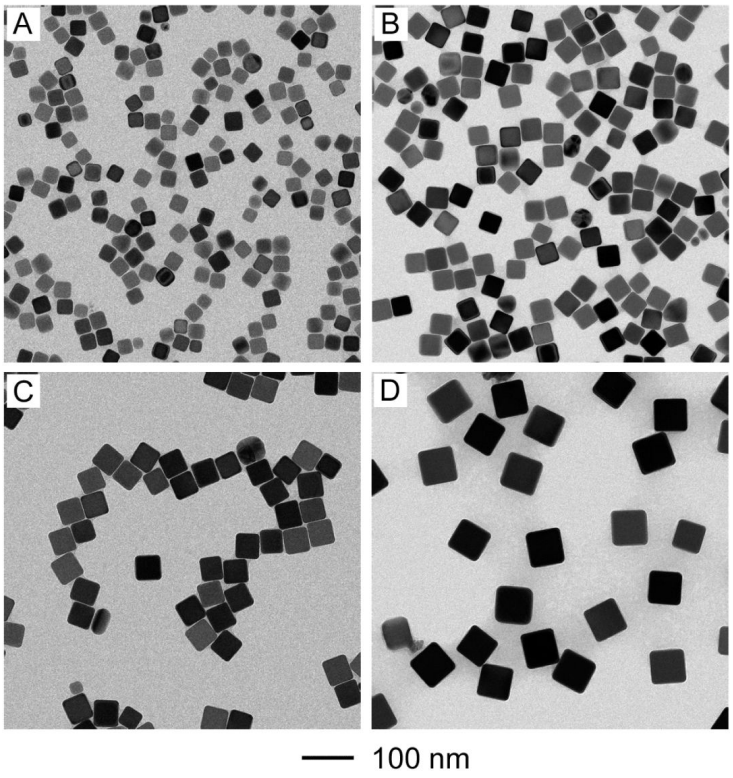

Figure 1.
TEM images of Ag nanocubes at different reaction times for a standard synthesis: (A) 15, (B) 30, (C) 60, and (D) 90 min. The nanocubes have an edge length of (A) 30, (B) 42, (C) 50, and (D) 70 nm.

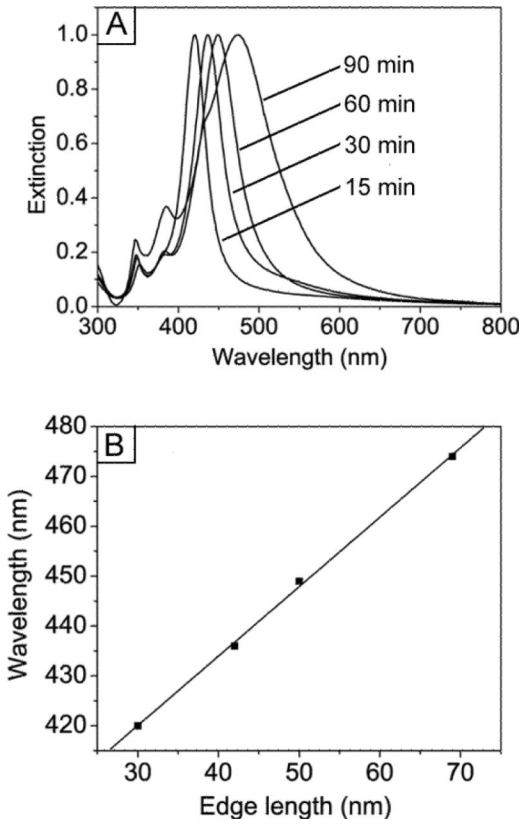

Figure 2.

Fine control of the edge length of Ag nanocubes based on the UV-vis spectroscopy. (A) UV-vis spectra taken from the aqueous suspensions of Ag nanocubes shown in Figure 1. (B) Calibration curve showing the linear dependence between the major localized surface plasmon resonance (LSPR) peak position and the edge length of Ag nanocubes.

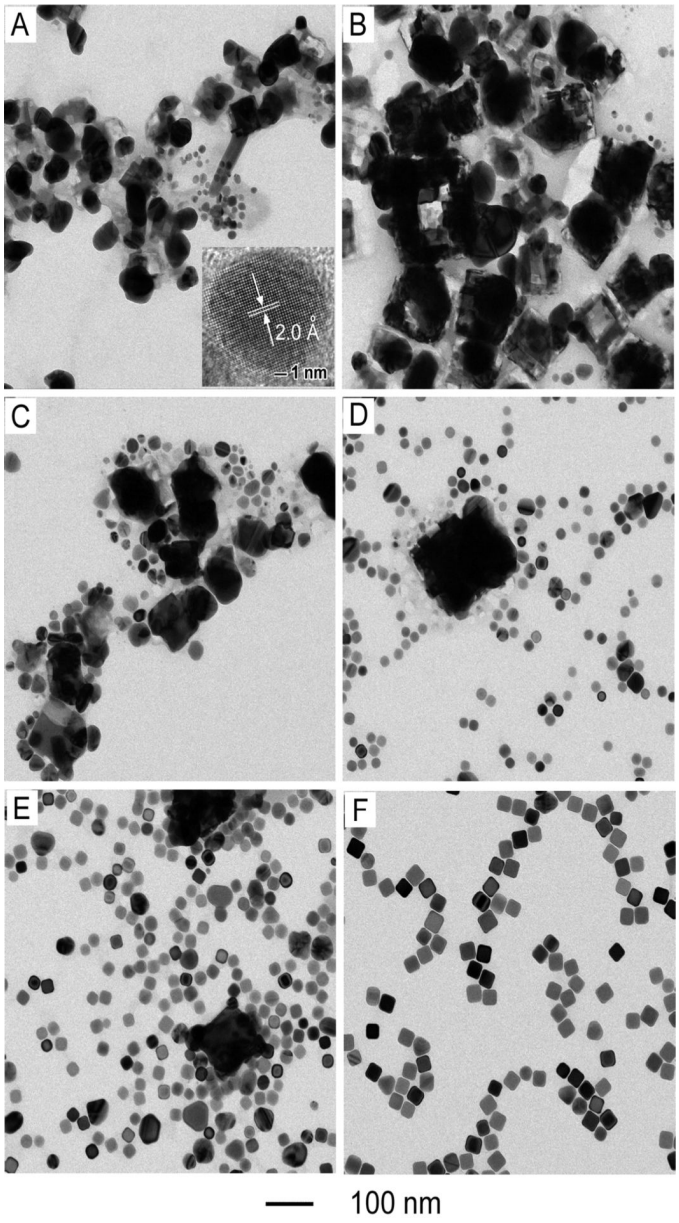

Figure 3.
TEM images of six aliquots taken from different stages of a standard synthesis: (A) 1, (B) 3, (C) 5, (D) 9, (E) 11, and (F) 15 min. HRTEM image of the small Ag nanoparticles shown in the inset taken from the sample at t = 1 min.

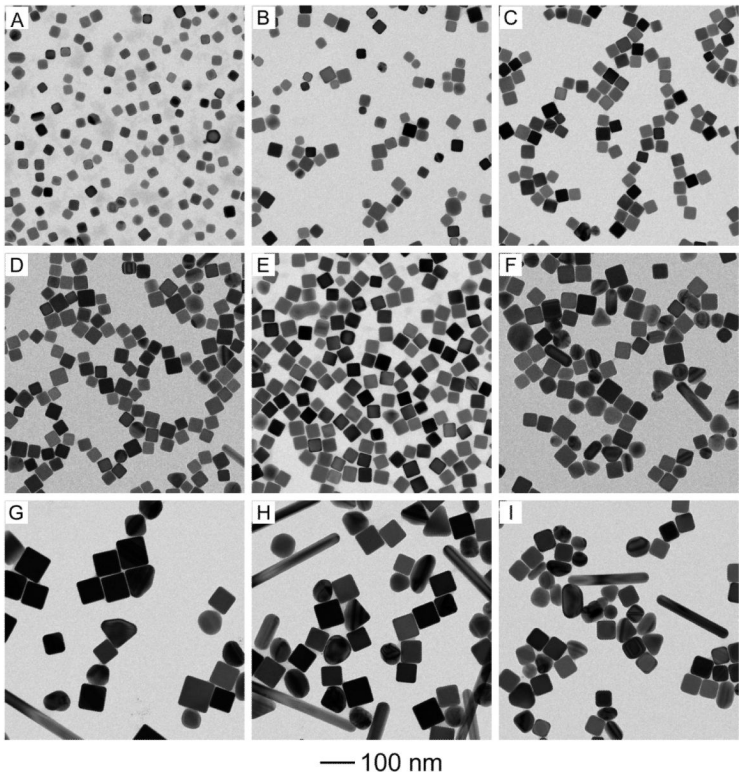

Figure 4.

TEM images of Ag nanoparticles from a series of synthesis when the concentration of NaHS was varied from 12 to 25 and 50 μM (from left to right), and the concentration of HCl was increased from 0.10 to 0.21 and 0.42 mM (from the top to bottom). Each row shows reactions that were performed under the same concentration for HCl, and each column under the same concentration for NaHS. All other parameters were kept the same as the standard synthesis.

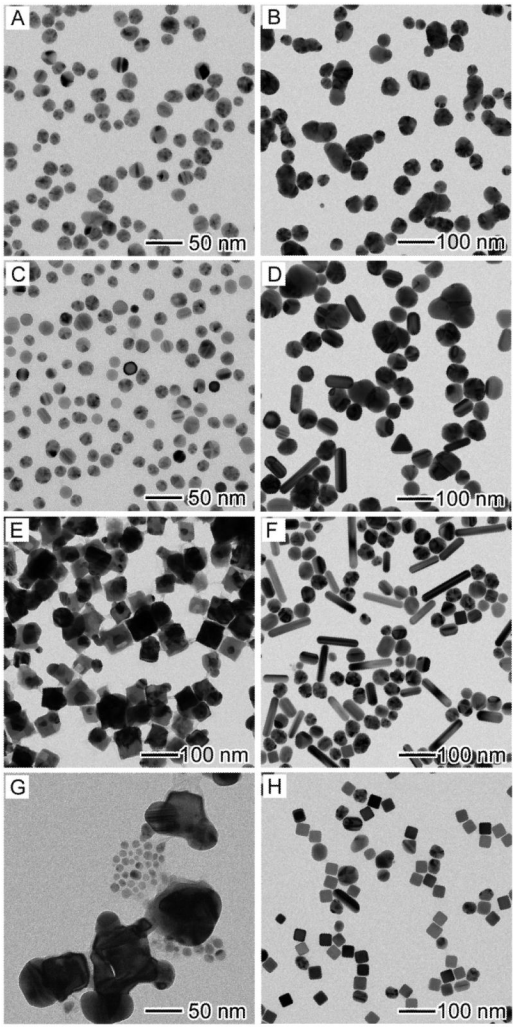

Figure 5.
TEM images of Ag nanoparticles obtained at t = 1 min (left column) and t = 30 min (right column) for the syntheses with different precursor combinations: (A, B) $C_3FCOOAg$; (C, D) $C_3FCOOAg$ + NaHS; (E, F) $C_3FCOOAg$ + HCl; and (G, H) $C_3FCOOAg$ + NaHS + HCl, but under argon atmosphere. All other parameters were kept the same as the standard synthesis.

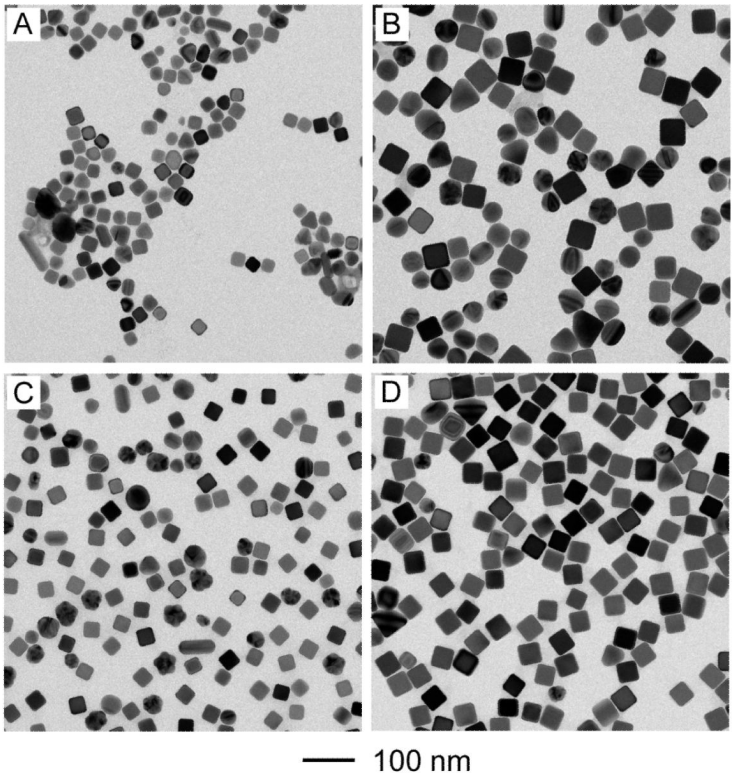

Figure 6.
TEM images of Ag nanocubes synthesized under different conditions: (A) at 13°C; (B) at 170 °C; (C) addition of NaCl instead of HCl; and (D) 20 × scale-up synthesis. All other parameters were kept the same as the standard synthesis.